Journal Name

Received 00th January 20xx,
Accepted 00th January 20xx

DOI: 10.1039/x0xx00000x

The spatial distribution of photostability of thionine confined in zeolite L nanochannels investigated by Photobleaching Lifetime Imaging Microscopy (PbLIM)

Diego Lencione, Marcelo H. Gehlen*, Loren N. Trujillo, Renan C. F. Leitao, and Rodrigo Q. Albuquerque*

Instituto de Química de São Carlos, Universidade de São Paulo, 13566-590 São Carlos – SP, Brazil

Dye photobleaching is a photochemical reaction that can be investigated locally by fluorescence microscopy techniques. In this study a user-friendly computational tool to assist photobleaching experiments called Photobleaching Lifetime Imaging Microscopy (PbLIM) is presented. With this tool it is possible to recover the photobleaching kinetics spatially, where a photobleaching lifetime is generated for each pixel of the image. Our model was applied to the photobleaching process of thionine encapsulated into the one-dimensional nano channels of Zeolite L (ZL), from where we gained insight on the molecular oxygen distribution inside ZL channels, as well as on the detailed photobleaching of the confined thionine.

Introduction

Photobleaching is a photochemical reaction of a dye or a fluorophore with surrounding molecules that turns it unable to perform cycles of fluorescence emission. Despite being a broadly investigated phenomenon, a few groups have investigated it locally, with the help of fluorescence microscopy techniques. The first ideas for imaging the photobleaching phenomena with an optical microscope date of the end of 1980 decade, with the contribution of Douglas M. Benson *et al.*[1] By acquiring a temporal sequence of fluorescence images, the authors had introduced the concept of an image where each pixel represents the rate of photobleaching in the sample, according to a previous exponential fitting process. In the sequence, other authors have developed new methods based on photobleaching imaging to determine the efficiency of fluorescence resonance energy transfer (FRET), as for example the acceptor photobleaching technique, with applications in the biological and health areas.[2,3,4] More recently, Sage and Wüster have developed an open-access computational tool called PixBleach, working as a plugin of the software ImageJ.[5] With this tool it is possible to image the photobleaching process by fitting the experimental data with a mono, bi or a stretched exponential decay functions. Nevertheless the investigation of increasingly more complex systems combined with the availability of powerful computational tools in different platforms allow the development of new tools to provide additional features and possibilities in photobleaching image analysis. This was the motivation to develop a new computational tool for photobleaching imaging and to apply it to access the spatial distribution of photostability of thionine entrapped in zeolite L (ZL).

Zeolite L is a largely used microporous material to design inorganic-organic hybrid systems.[6,7,8] This versatile aluminosilicate can be synthetized in different sizes (from nanometers to micrometers) and ratios, and its surface functionalization leads to new functional materials.[9] Different dyes can be encapsulated inside the one-dimensional channels of ZL[10], allowing energy transfer processes to be accurately described, as reported by Calzaferri *et al.*[11] Pina *et al*[6] have reported that photochemical reactions can also take place inside the channels of ZL. The framework and dimensions of the main entrance channel of ZL are displayed in Fig. 1.

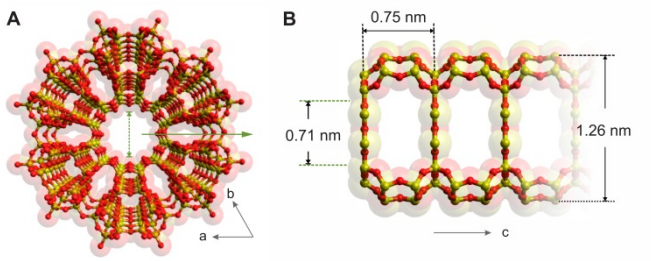

Fig. 1 (A) Top View of ZL framework highlighting the central 1D channel, (B) side view of one single channel revealing its dimensions.

Thionine, a visible light-absorbing molecule with heterocyclic planar structure and bearing a positive charge on the sulfur atom (Fig. 2), is one of the guest molecules which has been successfully inserted into the channels of ZL. Owing to the molecular dimension of this dye (0.72 x 1.5 nm) and space restrictions imposed by the geometry of ZL, thionine exists within the channels exclusively as a monomer.[13,14] Although geometric constraints in solid matrices may avoid the dye self-aggregation, resulting in an improvement of the dye photostability,[15,16] the entrapped thionine in ZL can still

*Corresponding authors: marcelog@iqsc.usp.br,rodrigo_albuquerque@iqsc.usp.br
† Electronic Supplementary Information (ESI) available: Matlab code request for PbLIM and its user interface image; optical layout for the wide field fluorescence setup; cross-section of the photobleaching decay; photobleaching lifetime images with the respective initial condition for the fluorescence. See DOI: 10.1039/x0xx00000x

undergo photoinduced changes promoted by the surrounding molecular environment, that quenches its fluorescence in an irreversible reaction. For instance, it is accepted that upon irradiation, the triplet excited state of thionine may be populated and, when in the presence of oxygen, it is able to transfer its energy, generating singlet oxygen ($^1O_2$).[17,18] The diffusion of the reactive $^1O_2$ inside the ZL can oxidize encapsulated dyes (eg. Thionine), causing their photobleaching.

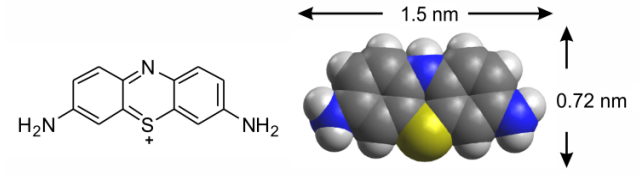

Fig. 2 Structure and dimension (van der Waals) of thionine guest molecule.

In this report, wide field fluorescence microscopy is used to generate photobleaching lifetime images of thionine encapsulated in ZL, allowing the visualization of its spatial distribution of photostability. The influence of the sample atmosphere (air and argon) and excitation irradiance on photostability patterns are also investigated. The results of thionine loaded in ZL are compared with the photobleaching of thionine embedded in a film of poly (vinyl pyrrolidone) (PVP). The analysis of the photobleaching lifetime images are used to give insights on the molecular oxygen distribution inside the ZL channels.

Materials and methods

Chemicals

Micrometer-sezed zeolite L crystals (average length / diameter = 5.25 / 2.0 µm) were obtained from the lab of Dr. Dominik Brühwiler. Thionin acetate salt (dye content ≥ 85%) was obtained from Sigma Aldrich. Hydrofluoric acid (48-50%) was acquired from Êxodo Científica (48-50%) and Ethanol (99.5%) was obtained from Synth. All solutions were prepared using deionized water. PVP with average molecular weight of 55,000 g mol^{-1} obtained from Sigma Aldrich was used to produce the polymeric thin films with thionine.

Sample preparation (µZeol-Thionine)

33 mg of ZL were suspended in 2 mL of deionized water and stirred under ultrasonic bath for 1 h to disperse aggregated crystals. Subsequently, 24 mL of an aqueous thionine solution (5.0 x 10^{-5} mol L^{-1}) were added to the ZL suspension followed by magnetic stirring at 100 °C for 24 h. After that, the suspension was centrifuged at 14,000 rpm for 20 min. The collected solid sample was washed and centrifuged successively with 2 mL of ethanol and deionized water until no thionine could be detected in the supernatants. The loading of thionine was obtained by the HF test.[19]

PVP films

1 mL of PVP solution at 15% in ethanol was mixed with 0.5 mL of thionine solution (10^{-5} mol L^{-1}) and stirred for 10 min. The thionine-PVP thin film was produced on a microscope coverslip by spin-coating 150 µL of the final mixture at 2,000 rpm for 1 min.

Description of the PbLIM software

The images and results presented in Fig. 3 is a target motivation to develop a new computational tool to assist dye photobleaching process. By observing individually a large number of ZL crystals homogeneously loaded with thionine, it has been found that generally the photobleaching rate in the border of the zeolites is higher than in its central part. To quantify this difference, the fitting with a mono-exponential function to determine the photobleaching lifetime in these regions has been performed. Specifically for the image in the Fig. 3A, the lifetime of the selected points was 48.8 s (border) and 69.3 s (center). Generalizing this concept, by fitting the whole experimental decay data pixel by pixel over the central plane of ZL crystal, a photobleaching lifetime image is created (Fig. 3C). The interesting pattern found in the spatial distribution of the photobleaching lifetime, apparently uncorrelated with the initial fluorescence intensity image, shown in Fig. 1a, motivated us to incorporate more features in our software to investigate this phenomenon more systematically. The PbLIM software was developed with the help of the graphical user interface environment of Matlab – Mathworks® and has some important features that differentiate it from the current state-of-the-art of photobleaching imaging, which are highlighted below:

i) A threshold level is used to select the region of interest in the initial fluorescence image to investigate the photobleaching kinetics;

ii) Mono or bi exponential decay functions to fit the experimental data. When the bi exponential function is selected, the average photobleaching lifetime is used to compose the image;

iii) There are two complementary ways to check the convergence of the fitting process. The first check is a local verification, where a point in the image is chosen by the user and the fitting residuals are presented as a function of time, whereas the second one is a more general approach that generates an image with the standard deviation of the fitting process across the selected region used to investigate the photobleaching kinetics.

With the help of these features the user has quantitative elements to define the appropriate exponential fitting model. Furthermore, besides generating photobleaching lifetime images, the software calculates the average photobleaching lifetime value and its standard deviation, which can be very useful for a comprehensive study of the sample behavior under different experimental conditions. The software has also a graphical user interface with saving and exporting features

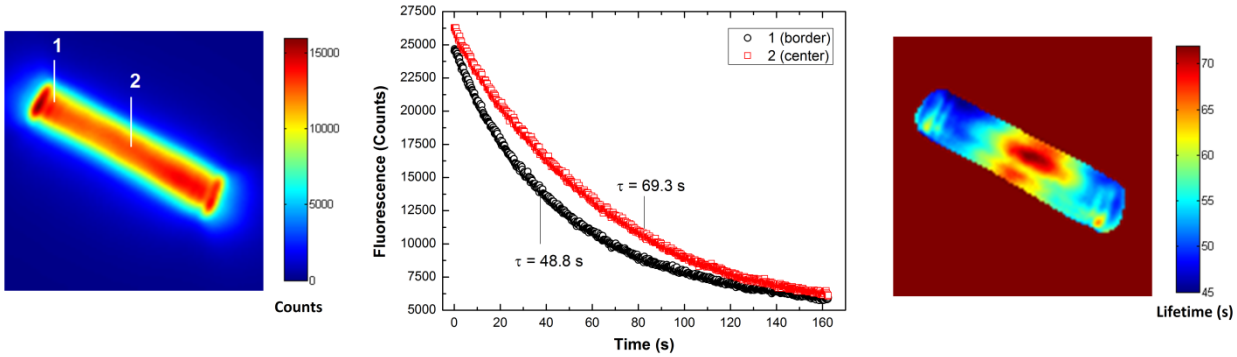

Fig. 3 Photobleaching process of thionine hosted in zeolite L in air atmosphere. A homogeneous distribution of dyes in the channels of the zeolite can be seen in the wide field fluorescence image presented in (A). Points 1 and 2 have the photobleaching decays shown in (B). where the lifetime values were fitted using mono-exponential decay function. Applying this procedure to all pixels of the image (A) results in the photobleaching lifetime image shown in (C), where the value of each pixel represents its respective photobleaching lifetime. The window size for both images, (A) and (C), is 8.5 x 8.5 µm.

for all the generated results. More details about the software capabilities are available in the electronic supplementary information (ESI†).

When a mono exponential decay function is selected to fit the decay data the following expression is used:

$$I_{ij}(t) = A_{ij} + B_{ij}exp(-C_{ij}t) \quad (1)$$

where ij represents the pixel position, t is time, A is an offset used to compensate for the background signal or minimum scattered light reaching the detector, B is the amplitude and C is the local rate of photobleaching, the inverse of photobleaching lifetime τ:

$$\tau_{ij} = {}^{1}/_{C_{ij}} \quad (2)$$

For a bi-exponential fitting, equation (3) is used:

$$I_{ij}(t) = A_{ij} + B_{ij}exp(-C_{ij}t) + D_{ij}exp(-E_{ij}t) \quad (3)$$

The two lifetimes are defined by: $\tau_{ij}(1) = {}^{1}/_{C_{ij}}$ and $\tau_{ij}(2) = {}^{1}/_{E_{ij}}$. Using this fitting function, the average lifetime quantifying the photobleaching kinetics is calculated by:

$$\langle\tau\rangle_{ij} = \frac{B_{ij}\,\tau_{ij}(1)^2 + D_{ij}\tau_{ij}(2)^2}{B_{ij}\,\tau_{ij}(1) + D_{ij}\,\tau_{ij}(2)} \quad (4)$$

In addition, from the plot of residuals of the fitting process the user can evaluate which decay function better describes the photobleaching kinetics.

Experimental setup

The fluorescence images were obtained in an inverted microscope, IX71 – Olympus, optically adapted to operate in wide field mode. Samples were excited at 532 nm by a CW model VERDI – Coherent laser, operating at low power, with circular polarization laser beam properly adjusted by using λ/2 and λ/4 waveplates, models AHWP05M-600 and AQWP05M-600 – from Thorlabs. The excitation beam was adjusted to 532 ± 2 nm with a band pass filter FLH5323-4 from Thorlabs. To separate the fluorescence signal from the excitation light a dichroic filter model model Z532rdc – Chroma and a notch filter NF01-532U-25 from Semrock were used, thus eliminating all the scattered photons generated in the excitation path. The samples were focused with an objective with 100X magnification and NA = 1.49, model UAPON 100X – Olympus, operating with immersion oil, n_d= 1.515, Type DF – Cargille Laboratories. The fluorescence images were recorded with an EMCCD Peltier cooled camera model Evolve 512 – Photometrics. The camera was coupled in the left side port of the microscope using an optical system with a magnification of 1.9X, model 25-71-52 – Best Scientific. The frame rate of image acquisition was set to 15 fps. By calibrating the optical magnification we have found that one pixel of the image sensor represents 84 nm in the sample plane. The excitation irradiance was varied from 10 to 300 W cm^{-2} by tuning the optical power of the laser, measured with a power and energy meter model Nova – Ophir Optics, and using the optical head model 3A-P-V1. The Optical layout of the wide field fluorescence microscopy setup is illustrated in the ESI†.

All the components in the experimental setup were mounted in an optical table with active vibration isolation avoiding external mechanical impacts that could cause misalignment during the long term imaging acquisition process.

Results and discussion

The loading of thionine in the prepared samples was 2.25%, i.e., 2.25 % of the zeolite sites are occupied with dyes. For thionine, one site means two unit cells. Images obtained by Scanning Electron Microscope (SEM) indicate the hexagonal geometry (Fig. 4A) and the cylindrical shape (Fig. 4B) of the zeolite L crystals used in this study.

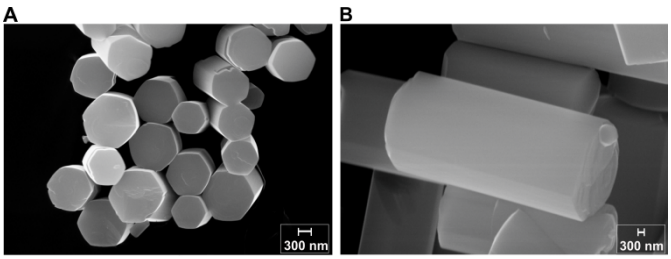

Fig. 4 Scanning Electron Microscope (SEM) of μZeol-L, front and size image, respectively.

Some differences in emission patterns are observed in the behavior of the photobleaching of thionine from one ZL microcrystal to another that can be explained by differences in the dye loading among the samples. For this reason, for each experimental condition used at least ten ZL microcrystals had their photobleaching kinetics monitored to generate the corresponding photobleaching lifetime images. In this way we are reporting a set of statistical results for the photobleaching process of the thionine-loaded ZL. The results are summarized in Figure 5, where, for each experimental condition, a representative photobleaching lifetime image is used to illustrate the typical spatial profile found. The numerical results reported in Fig. 5 are also plotted in Fig. 6, where the higher photostability found in low excitation irradiance for the experiments performed in argon atmosphere and the decrease of the photostability in both cases, in air and argon atmosphere, when increasing the excitation irradiance are clearly observed. The higher dye photostability in argon atmosphere and low irradiance suggests that the presence of molecular oxygen is an important factor in the photobleaching process. Considering that triplet excited state of thionine is formed from intersystem crossing of the singlet excited state, this species may react with oxygen to generate singlet oxygen ($^1O_2$) which in turn may produce direct or indirect oxidation of the dye leading to its photobleaching. Some clues about this effect can be found in the photobleaching lifetime image patterns observed when the experiments are performed in air equilibrated condition. The entrances of the ZL channels have a higher renewal of molecular oxygen by the diffusion of oxygen from the air, making this region less photostable when compared with the center of the microcrystal. In some samples this effect generates symmetric pattern of lifetime with respect to the cylinder geometry of the ZL crystals. These ideas will be explored later in the section "Oxygen mapping".

To show how much the local environment can change the photostability of the dye, the average photobleaching lifetime of thionine hosted in ZL was compared with thionine homogeneously dispersed in a thin PVP film. The polymeric films exhibit a much smaller photostability, as can be seen in Fig. 6. The average photobleaching lifetime of the thionine was about five times higher when hosted in zeolites than when immobilized in the PVP film. For low excitation irradiance levels of the order of 10 W cm^{-2}, the thionine hosted in ZL has an average photobleaching lifetime of 72 s while the dye in PVP film reached a value of 15 s. This difference in lifetime increases with irradiance levels.

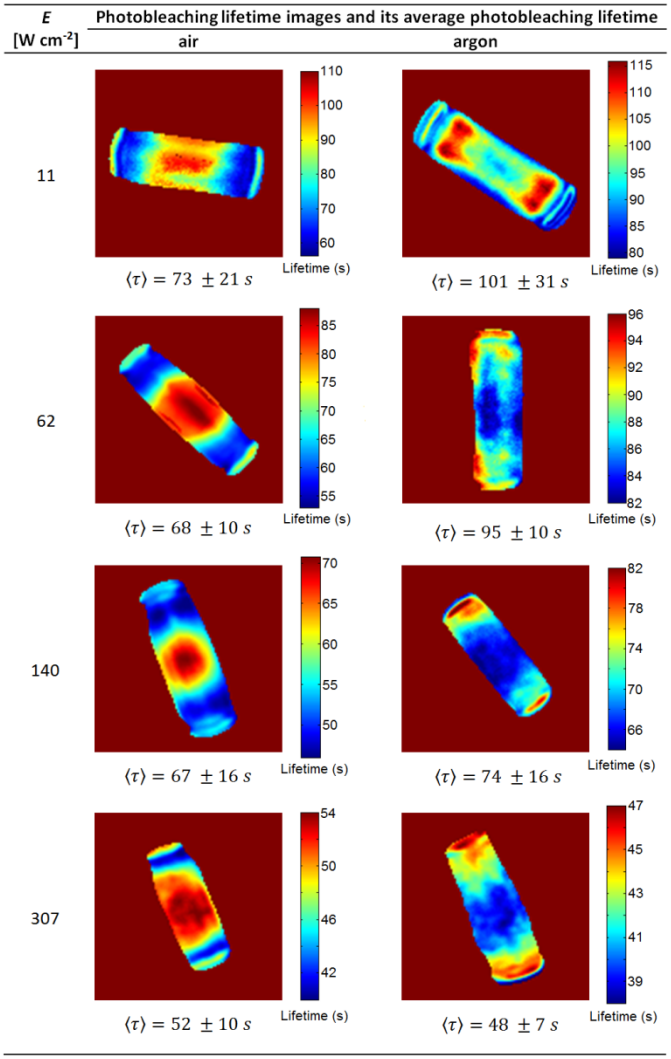

Figure 5 Examples of photobleaching lifetime images of thionine-ZL as a function of the excitation irradiance in air and argon atmospheres. For each experimental condition at least ten ZL crystals were analyzed. The average photobleaching lifetime and its standard deviation are also presented. The window size for all images is 8.5 x 8.5 μm.

Photobleaching kinetics

The PbLIM software was also useful to determine the photobleaching kinetics. For low excitation irradiances (below 80 W cm^{-2}), the photobleaching of thionine in zeolites can be well described by an exponential decay function, characterizing a first order kinetics. Above this level and below 310 W cm^{-2} (the maximum irradiance used in our experiments), a bi-exponential decay was necessary to fit the decay data, indicating a more complex kinetics in photobleaching. Fig. 7 illustrates this behavior, where photobleaching decay is monitored with mono and bi exponential functions under excitation irradiance of 11 W cm^{-2} and 307 W cm^{-2} respectively.

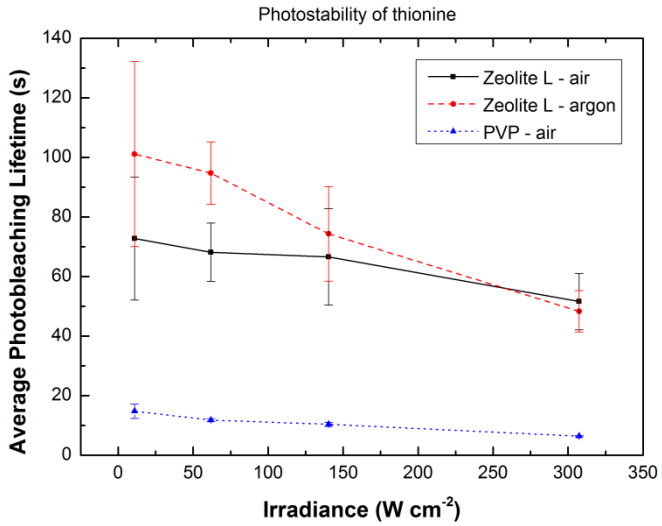

Fig. 6 Average photobleaching lifetime of thionine hosted in zeolite L and homogeneously dispersed in PVP film as a function of excitation irradiance in air and argon atmosphere.

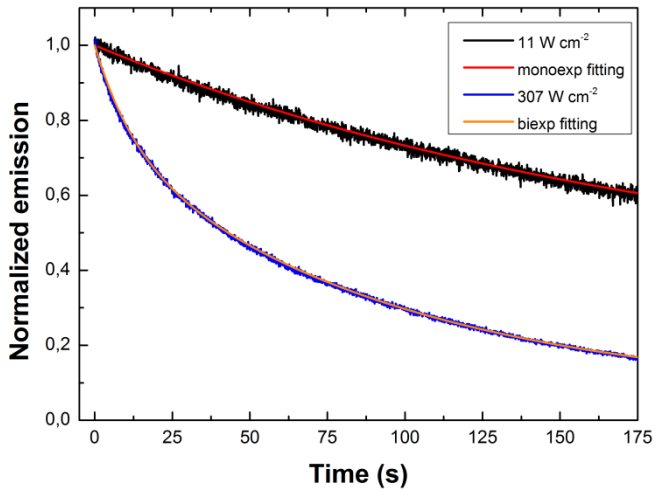

Fig. 7 Comparison of the photobleaching kinetics of thionine hosted in ZL under two levels of excitation irradiance (10.9 and 307 W cm^{-2}), fitted by a mono and bi exponential decay functions respectively.

Oxygen mapping inside the zeolite L

Due to the opposite symmetry found in the photobleaching lifetime images of the zeolites in air and argon atmospheres (Fig. 5), where the ends of the zeolite channels are less photostable than its center in air and the opposite in argon atmosphere, we are ascribing that, for low excitation irradiances where a first order photobleaching kinetics was verified, the local stationary concentration of molecular oxygen is playing a key role for the resulting spatial distribution of photostability. As described in the schematic model (Fig. 8), before starting experiments in air equilibrated condition it can be assumed that the zeolite channels were loaded with thionine and oxygen inside the ZL crystal. The regular fluorescence intensity profile of the zeolites shown in Fig. 3a supports the assumption of homogeneous dye distribution. Under constant excitation, the photobleaching process depletes both thionine and oxygen inside the channels. However, when irradiation is performed in air, the border of the zeolite will have much faster access to new oxygen coming from outside which would result in higher dye photobleaching rates at that region, as indeed observed. At the center of the crystals, after irradiation began, the depleted oxygen takes much more time to be substituted by new oxygen to continue the oxidation of entrapped dye molecules. One must keep in mind that each single unit cell of ZL has up to 3.6 exchangeable counter ions (here, K^+), about 21 water molecules if the crystal is fully hydrated[22] and, if the unit cell is part of an occupied dye site, there should be still place for half thionine. All these obstacles hamper the oxygen to the center of the ZL crystals and this increases the photostability in that region.

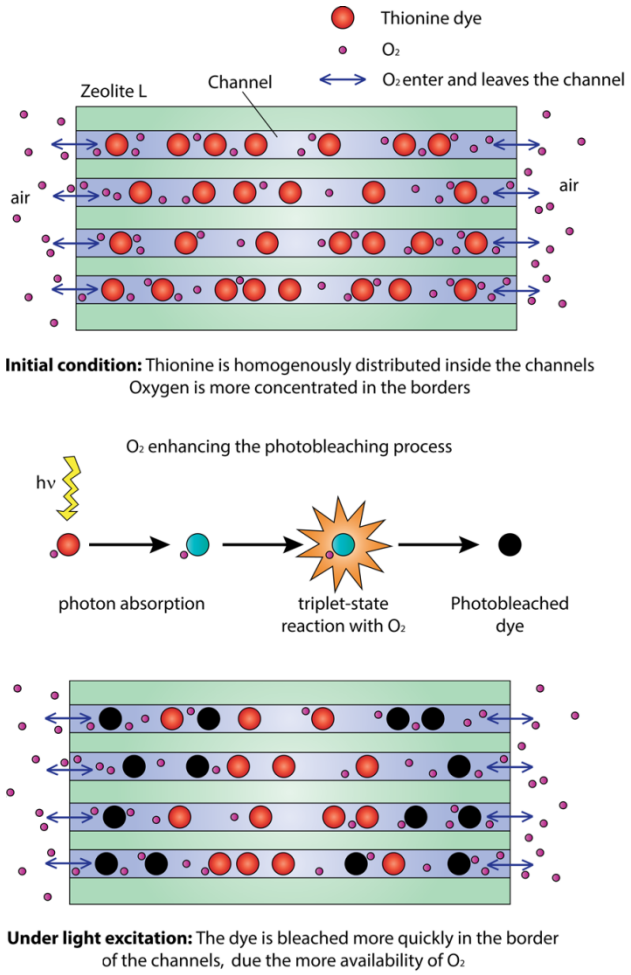

Fig. 8 Schematic model for the effect of oxygen as an accelerator component in the photobleaching kinetics of thionine hosted in zeolite L under low excitation irradiance. The higher availability of oxygen in the channel ends turns this region less photostable in air atmosphere.

At low excitation intensity the photobleaching follows an exponential decay with a lifetime defined by equation (2). Under assumption of photo-stationary concentration of oxygen the image recovery lifetime could be represented by:

$$\tau_{ij} = {}^{1}/_{C_{ij}} = (k_0 + k_1[O_2]_{i,j})^{-1} \quad (5)$$

Where $[O_2]_{i,j}$ represents the local photo-stationary concentration of oxygen in the lifetime image space and k_0 and k_1 are the intrinsic and oxygen-mediated dye photobleaching rates, respectively. Thus from a lifetime image the respective plot of the relative oxygen concentration may be obtained by inverting equation 5. This can provide an insight on how oxygen is distributed inside the monitored region. As an illustration, a typical PbLIM data is inverted to generate the corresponding relative oxygen map, as shown in Fig. 9.

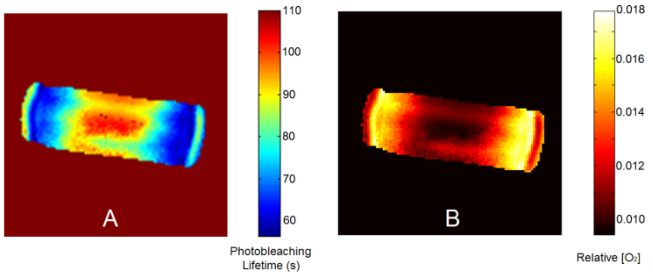

Fig. 9 The typical spatial distribution profile of the photobleaching lifetime image, **(A)**, give insights about the relative oxygen concentration inside the channels of zeolite L, **(B)**. The window size for both images is 8.5 x 8.5 µm.

The experiments made in argon atmosphere had their environment controlled at least one hour before the measurements. We interpret the spatial distribution of photobleaching lifetime showed in Fig. 5 (under argon) in the following way. The oxygen localized near the border of the ZL crystals channels is easily replaced by argon by diffusion, turning this region considerably more dye photostable, while the oxygen entrapped near to the center is partially blocked to diffuse out from the zeolite. In consequence, there is a residual oxygen concentration that turns the internal region less dye photostable. The convergence of the average photobleaching lifetimes found at higher excitation irradiance for both conditions (air and argon, see Fig. 6) suggests that second order effects due to the higher density of dye in excited state and the possibility of re-excitation of the same dye several times during long light exposure overcome the primary effect of the oxygen observed at low-irradiance experiments.

Conclusions

Dye photobleaching is an interesting and complex phenomenon that can be studied by combining powerful techniques of fluorescence microscopy. In this report a new computational tool, called PbLIM, to map the spatial distribution of photostability of materials is presented. To illustrate the use of this image tool, the spatial distribution of photostability of the thionine dye hosted in zeolite L and when homogeneously dispersed in a thin PVP film and varying the excitation irradiance in air equilibrated or argon atmospheres, has been investigated. The photostability was higher in zeolite crystals when comparing with the PVP film, as well as under low excitation irradiance levels and in argon atmosphere. The zeolites are recognized as systems that can increasing the photostability of hosted dyes,[20,21] however there was no previous study showing the spatial distribution of photostability of dyes in these materials. It has been shown here that the zeolite L homogeneously loaded with thionine exhibits a symmetric dye photostability profile, being more photostable in its center and gradually less photostable towards the edges. Oxygen seems to play a key role for the thionine photostability. The symmetry found in the spatial distribution of photostability of ZL-thionine is attributed to the inhomogeneity distribution of oxygen inside the channels after irradiation. The presence of a region of lower photostability at the center of the ZL crystal for experiments carried out in argon suggests that oxygen diffusion may be extremely slow in this kind of material.

Acknowledgements

MHG and DL thank FAPESP by the financial support 18215-6 that allowed the construction of the high resolution wide field fluorescence microscope. RQA thanks the funding from FAPESP (2012/2955-5) and CNPq (305082/2013-2). We are also grateful to Dominik Brühwiler for providing the micrometer-long zeolites.

Notes and references

1 D. M. Benson, J. Bryan, A. L. Plant, A. M. Gotto and L. C. Smith, Digital imaging fluorescence microscopy - spatial heterogeneity of photobleaching rate constants in individual cells, *J. Cell Biol*., 1985, **100**, 1309–1323

2 T. S. Karpova, C. T. Baumann, L. He, X. Wu, A. Grammer, P. Lipsky, G. L. Hager and J. G. McNally, Fluorescence resonance energy transfer from cyan to yellow fluorescent protein detected by acceptor photobleaching using confocal microscopy and a single laser, *J. Microsc.*, 2003, **209**, 56-70.

3 Y. Gu, L. Di, D. P. Kelsell and D. Zicha**,** Quantitative fluorescence resonance energy transfer (FRET) measurement with acceptor photobleaching and spectral unmixing, *J. Microsc***.,** 2004, **215**, 162-173.

4 E. B. van Munster, G. J. Kremers, M. J. Adjobo-Hermans and T. W. J. Gadella Jr., Fluorescence resonance energy transfer (FRET) measurement by gradual acceptor photobleaching, *J. Microsc.*, 2005, **218**, 253-262.

5 D. Wüstner, A. L. Larsen, N. J. Faergeman, J. R. Brewer and D. Sage, Selective Visualization of Fluorescent Sterols in Caenorhabditis elegans by Bleach-Rate-Based Image Segmentation, *Traffic* 2010, **11**, 440-454.

6 R. Gomes, R. Q. Albuquerque, F. Pina, A. J. Parola and L. De Cola, Supramolecular host–guest flavylium-loaded zeolite L hybrid materials: network of reactions

of encapsulated 7,4'-dihydroxyflavylium, *Photochem. Photobiol. Sci.*, 2010, **9**, 991-995.

7 D. Brühwiler, G. Calzaferri, T. Torres, J. H. Ramm, N. Gartmann, L.-Q. Dieu, I. López-Duarte and M. V. Martínez-Díaz, Nanochannels for supramolecular organization of luminescent guests, *J. Mater. Chem.*, 2009, **19**, 8040-8067.

8 S. Suárez, A. Devaux, J. Bañuelos, O. Bossart, A. Kunzmann and G. Calzaferri, Transparent Zeolite–Polymer Hybrid Materials with Adaptable Properties, *Adv. Funct. Mater.*, 2007, **17**, 2298–2306.

9 J. El-Gindi, K. Benson, L. De Cola, H.-J. Galla and N. S. Kehr, Cell Adhesion Behavior on Enantiomerically Functionalized Zeolite L Monolayers, *Angew. Chem. Int. Ed*., 2012, **51**, 3716 –3720.

10 F. Cucinotta, Z. Popović, E. A. Weiss, G. M. Whitesides and L. De Cola, Microcontact Transfer Printing of Zeolite Monolayers, *Adv. Mater*., 2009, **21**, 1142–1145.

11 E. Fois, G. Tabacchi, A. Devaux, P. Belser, D. Brühwiler, and G. Calzaferri, Host–Guest Interactions and Orientation of Dyes in the One-Dimensional Channels of Zeolite L, *Langmuir*, 2013, **29**, 9188–9198.

12 G. Calzaferri, and N. Gfeller, Thionine in the cage of zeolite L, *J. Phys. Chem.* 1992, **96**, 3428-3435.

13 L. Gigli, R. Arletti, J. G. Vitillo, G. Alberto, G. Martra, A. Devaux, and G. Vezzalini, Thionine Dye Confined in Zeolite L: Synthesis Location and Optical Properties, *J. Phys. Chem. C*, 2015, **119**, 16156−16165.

14 V. Ramamurthy, D. R. Sanderson, and D. F. Eaton, Control of dye assembly within zeolites: role of water, *J. Am. Chem. Soc.*, 1993, **115**, 10438-10439.

15 A. Dubois, M. Canva, A. Brun, F. Chaput, and J-P. Boilot, Photostability of dye molecules trapped in solid matrices, *Appl. Opt.*, 1996, **35**, 3193–3199.

16 G. Schulz-Ekloff, D. Wöhrle, B. van Duffel, R. A. Schoonheydt, Chromophores in porous silicas and minerals: preparation and optical properties, *Microporous Mesoporous Mater.*, 2002, **51**, 91-138.

17 A. Rodriguez-Serrano, V. Rai-Constapel, M. C. Daza, M. Doerr, and C. M. Marian, A theoretical study of thionine: spin–orbit coupling and intersystem crossing, *Photochem. Photobiol. Sci.*, 2012, **11**, 1860-1867.

18 S. Jockusch, J. Sivaguru, N. J. Turro and V. Ramamurthy, Direct measurement of the singlet oxygen lifetime in zeolites by near-IR phosphorescence, *Photochem. Photobiol. Sci.* 2005, **4**, 403–405.

19 Z. Li, G. Luppi, A. Geiger, H.-P. Josel, and L. De Cola, Bioconjugated Fluorescent Zeolite L Nanocrystals as Labels in Protein Microarrays, *Small*, 2011, **7**, 3193–3201.

20 R. Hoppe, G. Schulz-Ekloff, D. Wohrle, C. Kirschhock and H. Fuess, Location and photostability of faujasite-incorporated methylene blue, *Stud. Surf. Sci. Catal.*, 1994, **84**, 821-827.

21 G. Schulz-Ekloff, Nonlinear optical effects of dye-loaded molecular sieves, *Stud. Surf. Sci. Catal.,* 1994**, 85**, 145-175.

22 G. Calzaferri, S. Huber, H. Maas, C. Minkowski, Host-Guest Antenna Materials, *Angew. Chem. Int. Ed.* 2003, **42,** 3732-3758.

Supplementary information

The spatial distribution of photostability of thionine confined in zeolite L nanochannels investigated by Photobleaching Lifetime Imaging Microscopy (PbLIM)

Diego Lencione, Marcelo H. Gehlen*, Loren N. Trujillo, Renan C. F. Leitao and Rodrigo Q. Albuquerque*

* Instituto de Química de São Carlos, Universidade de São Paulo, CEP: 13560-590 São Carlos, Brazil;

* Corresponding authors

E-mail: marcelog@iqsc.usp.br

E-mail: rodrigo_albuquerque@iqsc.usp.br

1. **Matlab code files for PbLIM can be obtained by requesting via e-mail to Diego Lencione:** diego.lencione@gmail.com

2. **Optical layout**

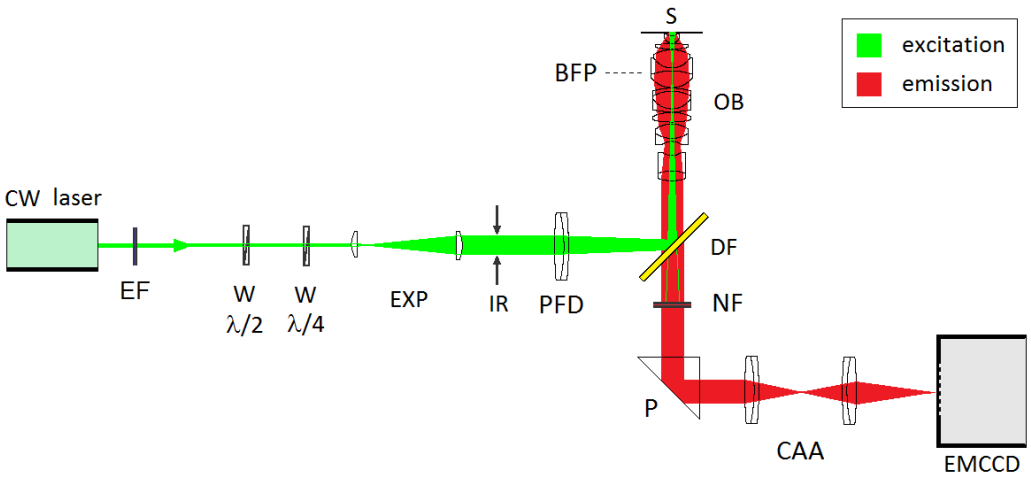

Fig. 10 Optical layout of the wide field fluorescence microscopy setup. BFP: objective back focal plane, CAA: camera coupling assembly, DF: dichroic filter, EF: excitation filter (narrow band pass filter), EXP: beam expander, IR: iris diaphragm, NF: notch filter, OB: objective, P: prism, PFD: pre-focusing doublet, S: sample, W: wave plate.

3. PbLIM software user interface

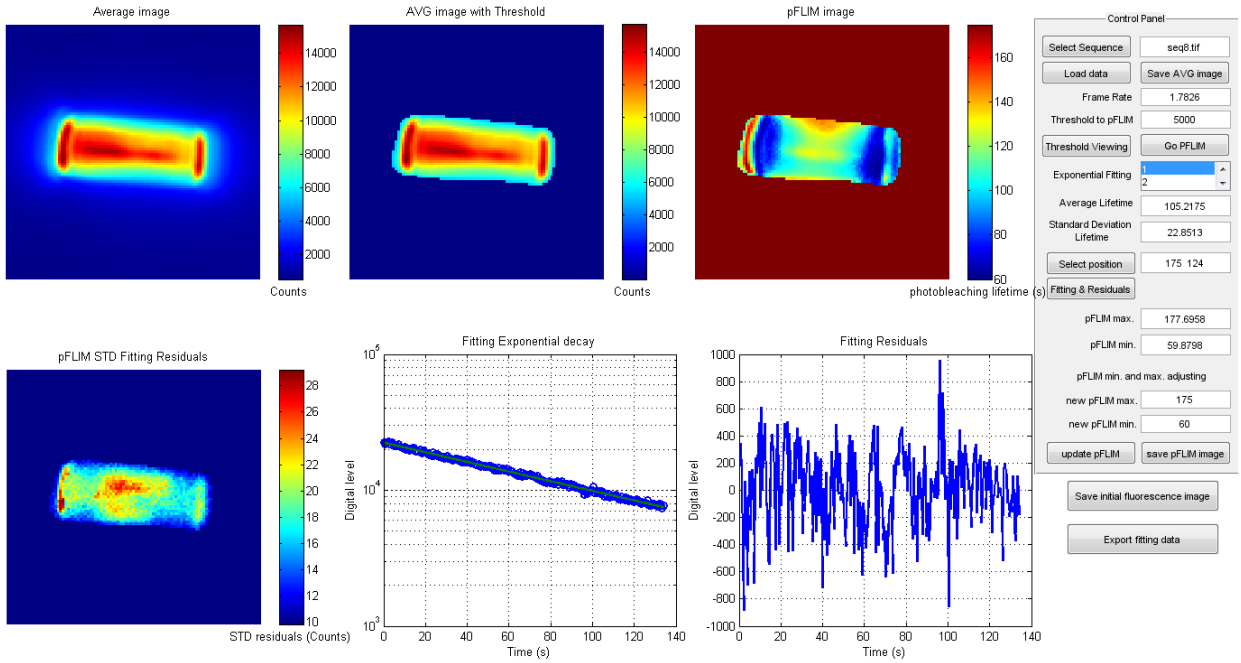

Fig. 11 User interface of the PbLIM software, showing typical results for a zeolite L.

4. Cross-section of the photobleaching decay

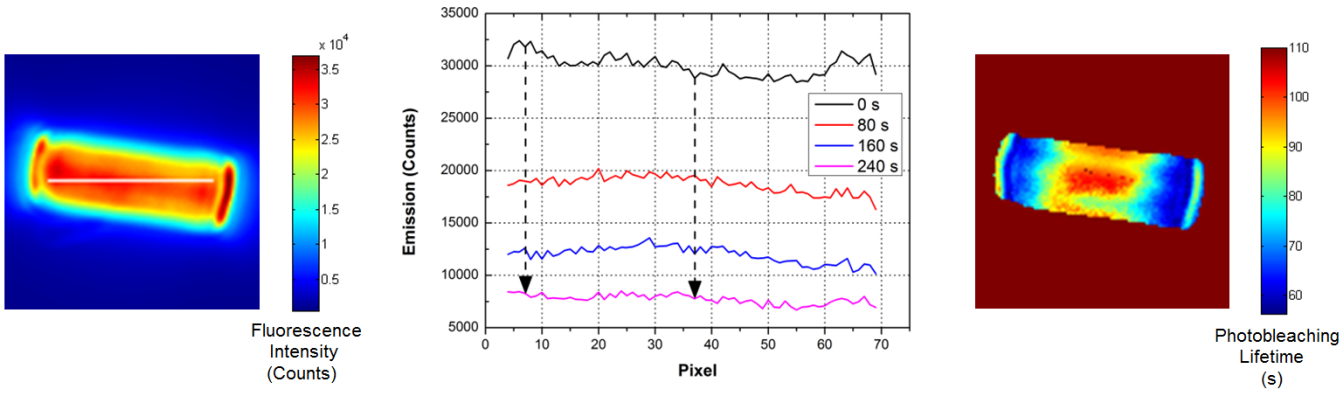

Fig. 12 Cross-section of the photobleaching decay in a zeolite L hosted with thionine under irradiance of 11 W cm^{-2}. **(Left)** Initial condition of the fluorescence, where the cross-section appears in white; **(Center)** Time-evolution of the fluorescence intensity in the selected cross-section; **(Right)** Resulting photobleaching lifetime image generated by mono exponential fitting.

5. Photobleaching lifetime images in different initial conditions

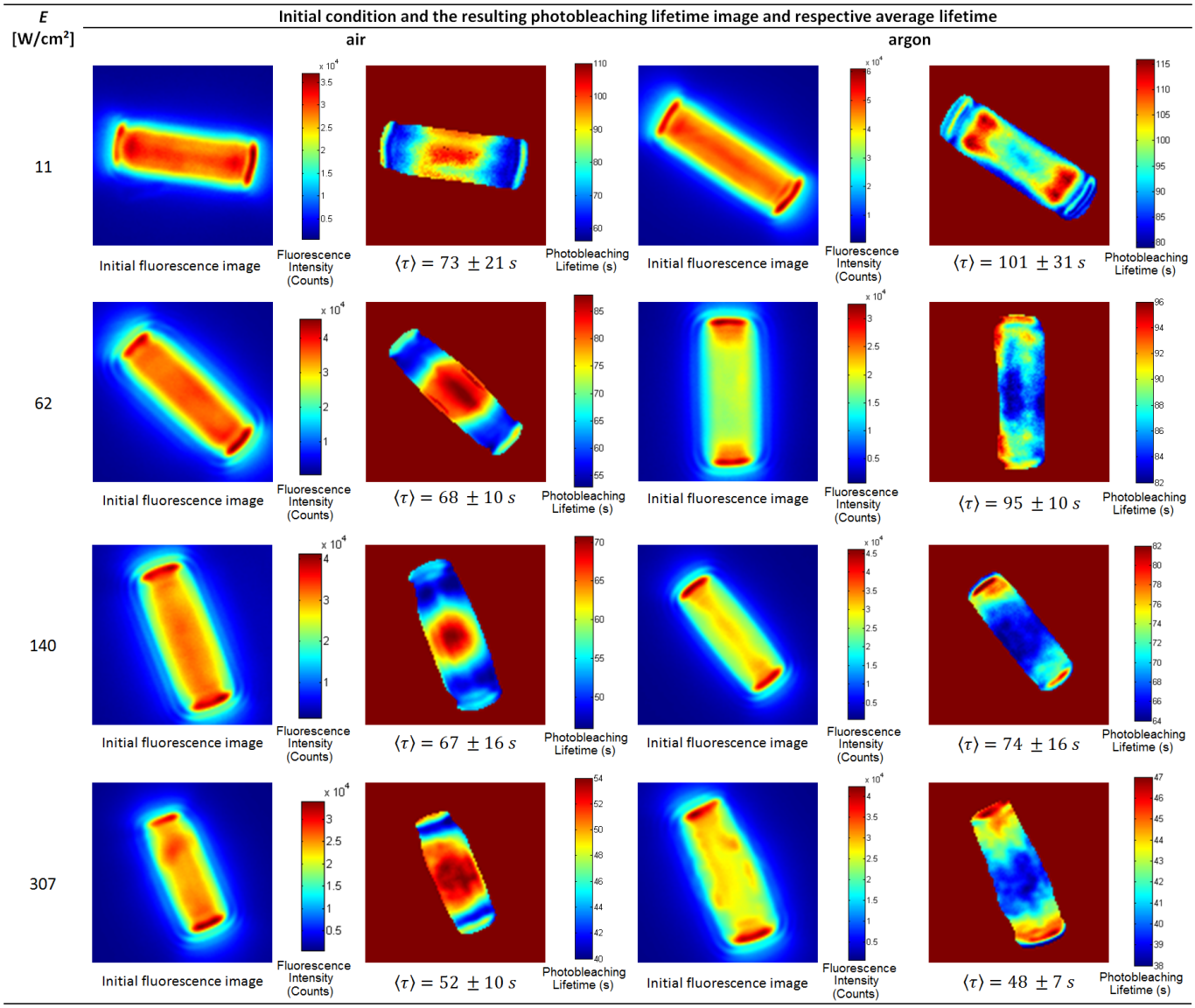

Figure 13 Photobleaching lifetime images of zeolite L hosted with thionine as a function of excitation irradiance in air and in argon atmosphere. For each experimental condition at least ten zeolites were analyzed individually, and the average photobleaching lifetime and its standard deviation are presented. The window of each image represents a square with side of 8.5 µm.